

Tree height and hydraulic traits shape growth responses across droughts in a temperate broadleaf forest

Ian McGregor, Ryan Helcoski, Norbert Kunert, Alan Tepley, Erika Gonzalez-Akre, Valentine Herrmann, Joseph Zailaa, Atticus Stovall, Norman Bourg?, William McShea?, Neil Pederson, Lauren Sack, Kristina Anderson-Teixeira

Title page

Title:

Authors:

| text | word count | other | n |
|--|---|------------------------------------|-----------------|
| Total word count (excluding summary, references and legends) | currently ~6000 (strict limit 6,500) | No. of figures | 2 (both colour) |
| Summary | ## (limit 200) | No. of Tables | 5 |
| Introduction | currently ~1536 | No of Supporting Information files | ###. |
| Materials and Methods | currently ~1442 | | |
| Results | currently ~1437 | | |
| Discussion | currently ~1881 (limit 30% of total (not strict), or 1950 if manuscript reaches word limit) | | |
| Acknowledgements | ~75 unwritten | | |

Summary (needs work)

- As the climate changes, driving increased drought in many forested regions around the world, mechanistic understanding of factors conferring drought vulnerability and resistance in trees is increasingly important. Yet it remains unclear how tree size and species' traits interactively shape tree growth responses across droughts.
- In this study, we analyze tree-ring records for 12 species representing 97% of woody productivity in the 25.6-ha ForestGEO plot in Virginia (USA) to determine how tree size, microhabitat, and species' traits interactively shape drought responses across the three strongest droughts over the 60 year period from 1950 and 2009.
- Individual-level growth responses to the three individual droughts were stronger in three cases: taller trees, trees in wetter microsites, and more drought-sensitive species as assessed by leaf traits (turgor loss at less negative leaf water potential, greater shrinkage with leaf dehydration). However, there was substantial variation in the best predictor variables across given droughts.
- We conclude that when droughts occur, tall trees, drought-sensitive species, and individuals in wetter microhabitats tend to be most strongly affected.

The Summary for research papers, which must be usable as a stand-alone document, must not exceed 200 words and should be organized using four bullet points to indicate: (1) the research conducted, including the rationale, (2) methods, (3) key results, and (4) the main conclusion, including the key points of discussion. It should not contain citations of other papers.

Key words: canopy position; drought; Forest Global Earth Observatory (ForestGEO); hydraulic traits; temperate broadleaf deciduous forest; tree growth; tree height; tree-ring [5-8] *Five to eight key words (in alphabetical order) . Words that are in the title can, and should, be among these. Very short phrases and scientific names with their common equivalents (e.g. *Nicotiana tabacum* (tobacco)) are acceptable.*

Introduction

Forests globally play a critical role in climate regulation (Bonan, 2008), yet there remains enormous uncertainty as to how the terrestrial carbon (C) sink, which is dominated by forests, will respond to climate change (Friedlingstein et al., 2006). An important aspect of this uncertainty lies in responses to drought (**REF**). In many forested regions around the world, the risk of severe drought is increasing (Trenberth et al., 2014), even in conjunction with increasing precipitation (Intergovernmental Panel on Climate Change, 2015). Global change-type drought has been affecting forests worldwide (Allen et al., 2010), and it is expected that future climate change-driven droughts will severely impact forests around the world (Allen et al., 2010); **REFS**). Larger trees tend to suffer more (e.g., Bennett et al. (2015); Stovall et al. (2019)), resulting in disproportionate impacts on forest C storage (Meakem et al., 2018). As a result, forest drought responses stand to strongly impact forest feedbacks to climate change (**REFS**), yet accurate characterization of drought responses remains a modeling challenge (**REFS**)—in part because some of the mechanisms underlying drought responses remain unclear. Understanding forest responses to drought requires increased functional understanding of how tree size, microhabitat, and species’ traits jointly confer individual-level vulnerability or resistance, and the extent to which their influence is consistent across droughts.

One fundamental question regarding forest responses to drought is what drives the observed tendency for large trees to suffer more during drought. Bennett et al. (2015) showed that in forests globally, large trees suffer greater growth reductions during drought, and numerous subsequent studies have reinforced this finding (Stovall et al., 2019; Hacket-Pain et al., 2016) **REFS**). However, this analysis quantified tree size based on DBH, which has no direct mechanistic meaning. This study proposed two major mechanisms—besides the tendency for bark beetles to preferentially attack larger trees (Pfeifer et al., 2011)—for the observed greater drought growth reductions of large trees. First, taller trees face greater biophysical challenge of lifting water greater distances against the effects of gravity and friction (McDowell et al., 2011; McDowell and Allen, 2015; Ryan et al., 2006; Couvreur et al., 2018), and this may become a greater liability during drought (Zhang et al., 2009). Second, larger trees may have lower drought resistance because they are more often in the canopy, where they are exposed to higher solar radiation, greater wind speeds, lower humidity, and lower CO_2 concentrations (**REFS-KAT**). Alternatively, the generally suppressed status of subcanopy trees may be insufficient to override the benefits of their buffered environment during drought. Potentially counteracting the biophysical challenges faced by large trees, their larger root systems may confer an advantage in terms of allowing greater access to water; however, it appears that this effect is usually insufficient to offset the costs of height and/or crown exposure (Bennett et al., 2015). A final mechanism that could mediate tree size-related responses to drought is how hydraulic traits are distributed with respect to size (Meakem et al., 2018). It is possible that the pattern observed by Bennett et al. (2015) could be caused if the larger size classes were dominated by species less adapted to handle drought, be it through avoidance, resistance, or resilience. Alternatively, larger size classes may be dominated by species that are better adapted to inherently greater biophysical challenges—as is the case in tropical moist forests of Panama, where larger size classes contain greater proportions of deciduous species (Condit et al., 2000; Meakem et al., 2018). Understanding the mechanisms underlying the tendency for larger trees to suffer more during drought will require sorting out the interactive effects of height, canopy position, root water access, and species’ traits.

A second fundamental question regarding forest responses to drought is how species’ traits – alone and in interaction with tree size – influence drought response. Xylem architecture plays a role, with diffuse porous species tending to be more drought-sensitive than ring-porous species (Kannenberg et al., 2019; Elliott et al., 2015; Friedrichs et al., 2009), but does not differentiate species beyond broad classes. Commonly-measured traits including wood density (WD) and leaf mass per area (LMA) have been linked to drought responses in temperate deciduous forests (Abrams, 1990; Guerfel et al., 2009; Hoffmann et al., 2011) and other forest biomes around the world (Greenwood et al., 2017). However, the direction of response is not always consistent; wood density correlated negatively with drought tree performance in a broadleaf deciduous forest in the southeastern United States (Hoffmann et al., 2011) but positively or with no effect at a global scale [Greenwood et al. (2017); Anderegg et al. (2018)]. Hydraulic traits including water potentials at which percent loss conductivity passes a certain threshold ($P50$, $P80$, $P88$) and hydraulic safety margin tend to be more successful at predicting drought performance (Anderegg et al., 2018) but are time-consuming to measure and therefore infeasible for predicting or modeling drought responses in highly diverse forests (e.g.,

in the tropics). More rapidly measurable leaf hydraulic traits with direct linkage to plant hydraulic function, including leaf area shrinkage upon dessication (PLA_{dry} ; (Scoffoni et al., 2014)) and turgor loss point (π_{tlp})—i.e., the water potential at which leaf wilting occurs (Bartlett et al., 2016) — are emerging as traits with potential to explain greater variation in plant distribution and function than the more commonly-measured traits such as WD and LMA (Medeiros et al., 2019). The ability of these hydraulic traits to explain tree performance under drought remains untested.

A final fundamental question regarding forest responses to drought is whether tree size and species’ traits have similar influence across droughts, or whether drought variability in factors such as severity, duration, and timing interact with tree size and traits such that different components of the community respond differently to different droughts. No two droughts are the same, and tree growth responses vary with drought characteristics such as timing and atmospheric demand (D’Orangeville et al., 2018). However, we are not aware of any studies that compare how tree size and species’ traits mediate growth responses across droughts. While tree-ring studies provide long-term records of tree responses to multiple droughts (e.g., (Lloret et al., 2011; D’Orangeville et al., 2018) **REFS**), these don’t test for differential trait effects across droughts (D’Orangeville et al., 2018) and generally focus on species-level responses, which preclude consideration of the roles of tree size and microenvironment. The ecological studies that have shaped our understanding of the role of tree size and microenvironment in forest drought responses generally examine only a single drought and tend to focus disproportionately on extreme droughts with dramatic impacts (e.g., (Allen et al. (2010); Bennett et al. (2015); Stovall et al. (2019); Anderegg et al. (2016)). Thus, our knowledge of forest responses to more modest but frequent droughts—e.g., those with historical return intervals on the order of a decade—remains more limited. While the tendency for larger trees to suffer more certainly predominates (Bennett et al., 2015), there are exceptions (e.g., **REFS**). There is also evidence that the degree to which larger trees suffer more increases with the severity of drought conditions (Bennett et al., 2015; Stovall et al., 2019). [*Are there any studies showing interactions of drought type with traits?*] Thus, while we expect many of the fundamental mechanisms shaping drought responses to be universal, we have little understanding of how tree size and traits interact with drought characteristics to result in differential responses across droughts.

Here, we combine tree-ring records covering three droughts (1966, 1977, 1999), species functional and hydraulic trait measurements, and forest census data from a 25.6-ha ForestGEO plot in Virginia (USA) to test a series of hypotheses and associated specific predictions (Table 1) designed to yield functional understanding of how tree size, microenvironment, and species’ traits collectively shape drought responses. First, we focus on the role of tree size and its interaction with microenvironment. We confirm that, consistent with most forests globally, larger-diameter trees tend to have lower drought resistance in this forest, which is in an ecoregion represented by only one study in (Bennett et al., 2015) (*H1.0*). We then test hypotheses designed to disentangle the relative importance of tree height (*H1.1*), crown exposure (*H1.2*), and root water access, which should be greater for larger trees in dry but not in perpetually wet microsites (*H1.3*). Second, we focus on the role of species’ functional and hydraulic traits and their interaction with tree height. We hypothesize that drought resistance will follow observed patterns in relation to wood density (negative effect; Hoffmann et al. (2011)) and specific leaf area (positive effect), but that hydraulic traits including xylem architecture (i.e., ring, semi-ring, or diffuse porous), leaf area shrinkage upon dehydration, and turgor loss point will prove better predictors (*H2.1*). We then test whether these traits correlate with tree height (*H2.2*), potentially driving the observed tendency for taller trees to suffer more during drought (*H2.3*). Finally, we focused on variability among droughts, asking how community resistance varied across droughts (*H3.1*) and whether the factors confirming vulnerability or resistance varied across droughts (*H3.2*).

Table 1. Summary of hypotheses, corresponding specific predictions, and results. We count predictions as fully supported / rejected when the response matches/contradicts the prediction in both univariate and all top multivariate models (when applicable). Parentheses indicate that predictions were partially supported/ rejected–i.e., that the direction of response matched/contradicted the prediction but that the effect was not significant in all models.

| Hypotheses & Specific Predictions | Prediction supported? | | | | Results |
|---|-----------------------|------------|-----------|------------|-------------------|
| | Overall | 1966 | 1977 | 1999 | |
| H1.0. Larger-diameter trees have lower drought resistance (R). | | | | | |
| 1.0 - R decreases with stem diameter. | yes | yes | (yes) | (no) | Table 4 |
| H1.1. Tall trees have lower drought resistance. | | | | | |
| 1.1 - R decreases with height (H). | yes | yes | (yes) | (no)/(yes) | Tables 4, 5 |
| H1.2. Trees with more exposed crowns have lower drought resistance. | | | | | |
| 1.2a - Dominant trees have lowest R. | (yes) | yes | (yes) | (no) | Tables 4, 5 |
| 1.2b - Correcting for H, dominant trees have lowest R. | (no) | (no) | (yes) | (no) | Tables 4, 5 |
| H1.3. Small trees (lower root volume) suffer more in drier microhabitats. | | | | | |
| 1.3 - There is a negative interactive effect between height and TWI. | (no) | (no) | (no) | (no) | Table 4 |
| H2.1. Species traits predict drought resistance. | | | | | |
| 2.1a - Wood density correlates negatively to R. | (yes) | (yes) | (yes) | (no) | Table 4 |
| 2.1b - Leaf mass per area correlates positively to R. | (yes) | (yes) | (no) | (yes) | Table 4 |
| 2.1c - Diffuse porous species have lower R than ring-porous. | (yes) | (yes) | (no) | yes | Tables 4, 5 |
| 2.1d - Percent loss leaf area upon desiccation (PLA) correlates negatively with R. | yes | yes | (yes) | (yes) | Tables 4, 5 |
| 2.1e - Turgor loss point correlates negatively with R. | (yes) | (yes)/(no) | (yes)/yes | (yes) | Tables 4, 5 |
| H2.2. At the community level, taller trees have more drought-resistant traits. | | | | | |
| 2.2a - Community mean wood density correlates negatively to H. | yes | - | - | - | Table S5 |
| 2.2b - Community mean leaf mass per area correlates positively to H. | yes | - | - | - | Table S5 |
| 2.2c - Community fraction of diffuse porous species decreases with H. | no | - | - | - | Table S5 |
| 2.2d - Community mean PLA correlates negatively to H. | no | - | - | - | Fig. 2e, Table S5 |
| 2.2e - Community mean turgor loss point correlates negatively to H. | no | - | - | - | Fig. 2f, Table S5 |
| H2.3. When traits are accounted for, taller trees still have lower drought resistance. | | | | | |
| 2.3 - R decreases with H when traits are included in the statistical model. | yes | yes | (yes) | (yes) | Table 5 |
| H3.1. Resistance differs across the droughts considered here. | | | | | |
| 3.1 - Drought year explains variation in R. | no | - | - | - | Fig. 1b, Table 4 |
| H3.2. The direction of responses to predictor variables differs across droughts. | | | | | |
| 3.2 - Directions of responses to best predictor variables differ across droughts. | rarely | - | - | - | Tables 4,5 |
| H3.3. The strength of responses to predictor variables vary across droughts. | | | | | |
| 3.3 - Best predictor variables differ across droughts. | yes | - | - | - | Table 5 |

Materials and Methods

Study site

Research was conducted at the 25.6 ha ForestGEO (Forest Global Earth Observatory) study plot at the Smithsonian Conservation Biology Institute (SCBI) in Virginia, USA (38°53'36.6"N, 78°08'43.4"W) (Bourg et al., 2013; Anderson-Teixeira et al., 2015a). SCBI is located in the central Appalachian Mountains at the northern edge of Shenandoah National Park. Elevations range from 273-338m above sea level (Gonzalez-Akre et al., 2016) with a topographic relief of 65m (Bourg et al., 2013). Dominant tree taxa include *Liriodendron tulipifera*, oaks (*Quercus* spp.), and hickories (*Carya* spp.).

Data collection and preparation

Within or just outside the ForestGEO plot, we collected data on a suite of variables including tree size, microenvironment, and species traits (Table 2). The SCBI ForestGEO plot was censused in 2008, 2013, and 2018 following standard ForestGEO protocols, whereby all free-standing woody stems ≥ 1 cm diameter at breast height (DBH) were mapped, tagged, measured at DBH, and identified to species (Condit, 1998). From this census data, we used measurements of DBH from 2008 to calculate historical DBH, tree location in the plot to determine the topographic wetness index, and data for all stems ≥ 10 cm to analyze functional trait composition relative to tree height (all analyses described below). Census data, which were last updated in 2019, are available through the ForestGEO data portal (www.forestgeo.si.edu).

Table 2x. Summary of variables

| variable | symbol | units | description | category | n | observed values | | | ln-transformed? |
|------------------------------|--------|--------|--|---|-------------------------|------------------|------------------|------------------|------------------|
| | | | | | | median | min | max | |
| Dependent variable | | | | | | | | | |
| drought resistance | R | - | ratio of growth during drought year to mean growth of the 5 years prior. | - | 1596 | 0.87 | 0 | 1.99 | no |
| Independent variables | | | | | | | | | |
| drought year | Y | - | year of drought | 1966 1977 1999 | 478 547 571 | - - - | - - - | - - - | - - - |
| <i>tree size</i> | | | | | | | | | |
| diameter breast height | DBH | cm | DBH in drought year | - | all | 31.92 | 3.92 | 134.19 | yes |
| height | H | m | H in drought year | - | all | 20.21 | 4.76 | 43.87 | yes |
| <i>microhabitat</i> | | | | | | | | | |
| crown position | CP | - | 2018 crown position | dominant (D) co-dominant (C) intermediate (I) suppressed (S) | 31 231 224 101 | - - - - | - - - - | - - - - | - - - - |
| topographic wetness index | TWI | - | steady-state wetness index based on slope and upstream contributing area | - | all | 5.66 | 0 | 16 | yes |
| <i>species' traits</i> | | | | | | | | | |
| wood density | WD | g cm-3 | dry mass of a unit volume of fresh wood | - | all | 0.62 | 0.4 | 1.09 | no |
| leaf mass per area | LMA | kg m-2 | ratio of leaf dry mass to fresh leaf area | - | all | 48.69 | 30.68 | 75.8 | no |
| xylem porosity | XP | - | vessel arrangement in xylem | ring semi-ring diffuse | 408 31 178 | - - - | - - - | - - - | - - - |
| turgor loss point | TLP | MPa | water potential at which leaves wilt | - | all | -2.39 | -2.76 | -1.92 | no |
| percent loss area | PLA | % | percent loss of leaf area upon desiccation | - | all | 13.06 | 8.52 | 24.64 | no |

We analyzed tree-ring data from 571 trees representing the twelve species contributing most to woody aboveground net primary productivity ($ANPP_{stem}$), which together comprised 97% of study plot $ANPP_{stem}$ between 2008 and 2013 (Helcoski et al., 2019) (Figure S1). Cores were obtained in 2010-2011 or 2016-2017 from a breast height of 1.3m using a 5mm increment borer. In 2010-2011, cores were collected from randomly selected live trees of species with at least 30 individuals of DBH ≥ 10 cm (Bourg et al., 2013). In 2016-2017, cores were collected from all trees found dead in the annual mortality census (Gonzalez-Akre et al., 2016). Cores were sanded, measured, and cross-dated using standard procedures, as detailed in (Helcoski et al., 2019). The resulting chronologies have been published in association with Helcoski et al. (2019): (ITRDB; GitHub/Zenodo). *Ryan submitted the data to ITRDB but I don't think its posted yet. We should also cite GitHub/Zenodo here. I'll come back to that.*

For each tree, we combined tree-ring records and allometric equations of bark thickness to retroactively calculate DBH for the years 1950-2009. Prior DBH was estimated using the following equation:

$$DBH_Y = DBH_{2008} - 2 * \left[\sum_{year=Y}^{2008} (r_{ring,Y} : r_{ring,2008}) - r_{bark,Y} + r_{bark,2008} \right]$$

Here, Y denotes the year of interest, r_{ring} denotes ring width derived from cores, and r_{bark} denotes bark thickness. Bark thickness was estimated from species-specific allometries based on the bark thickness data from the site (Anderson-Teixeira et al., 2015b). Specifically, we used linear regression equations on log-transformed data to relate bark thickness to diameter without bark from 2008 data (Table S1), which were then used to determine bark thickness in the retroactive calculation of DBH.

Height measurements (n=1518 trees) were taken by several researchers between 2012 to 2019, and are archived in a public GitHub repository. Measurement methods included manual (Stovall et al., 2018a, NEON), digital rangefinders (Anderson-Teixeira et al., 2015b), and automatic LiDAR (Stovall et al., 2018b). Rangefinders used either the tangent method (Impulse 200LR, TruPulse 360R) or the sine method (Nikon ForestryPro) for calculating heights. Both methods are associated with some error (Larjavaara and Muller-Landau, 2013), but in this instance there was no clear advantage of one or the other. Species-specific height allometries were developed (Table S2). For species with insufficient height data to create reliable species-specific allometries, heights were calculated from an equation developed using all height measurements.

Crown positions were recorded in the field during the growing season of 2018 following the crown position protocol of Jennings et al. (1999), whereby positions were ranked as dominant, codominant, intermediate, or suppressed. As there was no way to retroactively estimate crown position, we assumed that 2018 crown position was reflective of each tree’s position over the past 60 years. *While some trees undoubtedly changed position, an analysis of crown position relative to height (Fig. 2) and height change since the beginning of the study period indicated that change was likely slow. Specifically, average tree height growth was confined to <0.5m from 1966 to 1977, and ~1m from 1977 to 1999. (see issue #60).*

Topographic wetness index (TWI) was calculated using the dynatopmodel package in R (Figure S1) (?). Originally developed by Beven and Kirkby (1979), TWI was part of a hydrological run-off model and has since been used for a number of purposes in hydrology and ecology (Sørensen et al., 2006). TWI calculation depends on an input of a digital elevation model (DEM), and from this yields a quantitative assessment defined by how “wet” an area is, based on areas where run-off is more likely. From our observations in the plot, the calculation of TWI performed comparatively better at categorizing wet areas than the calculation of a distance matrix from a stream shapefile.

Hydraulic traits were collected at SCBI (Table 3). In August 2018, we sampled small sun-exposed branches from three individuals of each species in and around the ForestGEO plot. These were covered with opaque plastic bags, re-cut under water, and re-hydrated overnight before further analysis. Rehydrated leaves (n=3 per individual) were scanned, weighed, dried at 60° C for ≥ 48 hours, and then re-scanned and weighed. Leaf area was calculated from scanned images using an R script (**details - Valentine? Nobby?**). LMA was calculated as the ratio of leaf dry mass to fresh area. PLA was calculated as the percent loss of area between fresh and dry leaves. WD was calculated for ~1cm diameter stem samples (bark and pith removed) as the ratio of dry weight to volume. We used the rapid determination method of Bartlett et al. (2012) to estimate the turgor loss point (π_{tlp}). Briefly, two 4mm diameter leaf discs were cut from each leaf, tightly wrapped in foil, submerged in liquid nitrogen, perforated 10-15 times with a dissection needle, and then measured using a vapour pressure osmometer (VAPRO 5520, Wescor, Logan, UT, USA). Osmotic potential (π_{osm}) given by the osmometer was used to estimate (π_{tlp}) using the equation $\pi_{tlp} = 0.832\pi_{osm}^{-0.631}$ (Bartlett et al., 2012). We also characterized hydraulic vulnerability curves for the # most productive species, but because the water potentials at which 50% and 80% of conductivity is lost, $P50$ and $P80$, did not come out as top predictors in preliminary analyses and their inclusion limited the set of species that could be included in the full analysis, these traits were dropped from further consideration. Data and R scripts for hydraulic traits are available at [**create new public GitHub repo for hydraulic traits, archive in Zenodo, give DOI**].

To characterize how environmental conditions vary with height, data were obtained from the a National Ecological Observation Network (NEON) tower located <1km from the study area. We used data on wind

****Table 3.** Overview of analyzed species, their productivity in the plot, numbers and sizes sampled, and traits.**
Given are DBH mean and range of cored trees, the number of cores represented by each crown position of each species, and mean hydraulic trait measurements.

| species | mean.DBH_cm | DBH.range_cm | xylem.porosity | PLA_percent | LMA_g.per.cm2 | TLP_Mpa | WD_g.per.cm3 |
|---------|-------------|--------------|----------------|-------------|---------------|---------|--------------|
| caco | 27.2 | 50.8 | ring | 17.22 | 45.86 | -2.13 | 0.83 |
| cagl | 31.4 | 88.7 | ring | 21.09 | 42.76 | -2.13 | 0.62 |
| caovl | 35.3 | 51.1 | ring | 14.80 | 47.60 | -2.48 | 0.96 |
| cato | 21.0 | 20.1 | ring | 16.56 | 45.36 | -2.20 | 0.83 |
| fagr | 23.5 | 96.0 | diffuse | 9.45 | 30.68 | -2.57 | 0.62 |
| fram | 35.4 | 88.3 | ring | 13.06 | 43.28 | -2.10 | 0.56 |
| juni | 48.1 | 62.8 | semi-ring | 24.64 | 72.13 | -2.76 | 1.09 |
| litu | 36.9 | 90.4 | diffuse | 19.56 | 46.92 | -1.92 | 0.40 |
| qual | 47.2 | 67.7 | ring | 8.52 | 75.80 | -2.58 | 0.61 |
| qupr | 42.2 | 76.7 | ring | 11.75 | 71.77 | -2.36 | 0.61 |
| quru | 54.9 | 136.9 | ring | 11.01 | 71.13 | -2.64 | 0.62 |
| quve | 54.1 | 98.2 | ring | 13.42 | 48.69 | -2.39 | 0.65 |

speed, relative humidity, and air temperature, all measured over a vertical profile, for the years 2016-2018 (?). After filtering for missing and outlier values, the data was consolidated to represent the mean values per sensor height per day.

Identification of drought years

We identified droughts within the time period 1950-2009, defining drought (Slette et al., 2019) as events with widespread reductions in tree growth and anomalously dry peak growing season climatic conditions. Specifically, candidate drought years were defined as those where >25% of the cored trees experienced >30% reduction in basal area increment (BAI) relative to the previous 5 years, following the drought resistance (R) metric of (Lloret et al., 2011), and identified using the pointRes package (?) in R (version 3.5.3). Separately, we identified the years with driest conditions during May-August, which stood out in the analysis of (Helcoski et al., 2019) as the current-year months to which annual growth was most sensitive for trees at this site. We considered two metrics of moisture deficit: NOAA Divisional Data’s Palmer Drought Severity Index (PDSI) and the difference between monthly potential evapotranspiration (PET) and precipitation (PRE). These data were obtained from the ForestGEO Climate Data Portal (<https://github.com/forestgeo/Climate>) in August 2018, with monthly PET and PRE sourced from Climatic Research Unit high-resolution gridded dataset (CRU TS v.4.01; Harris et al. (2014)). The driest years were identified through simply ranking mean May-August PDSI or [PET-PRE] for the time period from driest to wettest.

Analysis

For each drought period, we calculated drought resistance (R) as the ratio of BAI during drought to that of the five previous years (Lloret et al., 2011). Analyses focused on testing the predictions presented in Table 1, most of which consider R as the response variable. The general statistical model for hypothesis testing was a mixed effects model (lme4 package from ?) with R as the response variable, tree nested within species as a random effect, and one or more independent variables as fixed effects. We used AICc (AICcmodavg package from ?) to assess model fit. Models were run for all drought years combined (with year as a fixed effect) and for each drought year independently. We first tested the predictor variables independently, counting a variable as useful for predicting R when AICc was reduced by ≥ 2 relative to the appropriate null model lacking that variable (Table 4). Because height had a substantial influence on R , we included it in the null model for testing other variables (Table 4).

Second, for each drought year and for all years combined, we determined the best multivariate models for predicting R . All variables with $dAICc > 1.0$ in any model (drought years combined or any individual drought) were used as candidate variables for each scenario’s best model. We compared models with all possible combinations of candidate variables and identified the full set of models within $dAICc=2$ of the top model (that with lowest AICc). These were counted as the “top multivariate models”. When a variable appeared in all of these top models and the sign of the coefficient was consistent across models, this was

counted as support for/ rejection of the associated prediction by the multivariate models. If the variable appeared in only some of the models, we considered this partial support.

Results

Focal droughts and their characteristics

In the 60-year period between 1950 and 2009, there were three droughts that met our criteria of anomalously dry climatic conditions coupled with substantial reductions in tree growth for at least some portions of the community: 1966, 1977, and 1999 (Figs. 1, S2). We excluded one year (1991) meeting the growth reduction criteria (26.5% of trees experienced $>30\%$ growth reduction, mean resistance = -13.8%) because this year was not among the driest in terms of May-August [PET-PRE] or PDSI (Table S3). Rather, the severity of growth reduction may be explained by defoliation by gypsy moths (*Lymantria dispar* L.) from approximately 1988-1995, which most strongly impacted *Quercus* spp. (Cite Shenandoah paper, if accepted). Climatically, these droughts included three of the five years between 1950 and 2009 with greatest moisture deficit (PET-PRE) during the peak growing season months of May-August, which are the months to which annual tree growth at this site is most sensitive (Helcoski et al., 2019). Specifically, 1966, 1977, and 1999 had mean MJJA PET-PRE of 83.37, 86.97, and 80 mm mo⁻¹, respectively. The years 1964 and 2007 also ranked in the top five driest (PET-PRE = 83.87 and 82.13 mm mo⁻¹), but were not among the lowest in terms of PDSI and were not identified as a pointer year (Table S3).

The droughts differed in intensity and prior onset (Table S3, Fig. S2). In terms of intensity during the peak growing season of the focal year, the 1999 drought was the most intense (lowest PDSI) during May-July. It was surpassed in intensity in August by the 1966 drought, which was otherwise the second most intense during the peak growing season. The 1977 was the least intense throughout the growing season. All droughts increased in intensity from May through August, but differed in the months previous. The 1966 drought was preceded by two years of moderate drought during the growing season and severe to extreme drought starting the previous fall. Similarly, the 1999 drought was preceded by severe to extreme drought starting the previous fall, but before that conditions were wetter than average until the previous June. The 1977 drought was preceded by 2.5 years of near-normal conditions, and was therefore the mildest of the three droughts by any measure.

Community-level tree growth responses to these droughts were modest, with modal resistance values of #, #, and # for 1966, 1977, and 1999, respectively (Fig. 1b). In each drought, roughly 30% of the cored trees suffered $\geq 30\%$ growth reductions ($R \leq 0.7$): 29.43% in 1966, 31.86% in 1977, and 26.81% in 1999. Some trees exhibited increased growth: ($R > 1.0$): 26.31% in 1966, 21.92% in 1977, and 25.57% in 1999.

Tree size and drought resistance

Overall, our analysis confirmed the tendency for larger-diameter trees to show greater reductions in growth during drought (Bennett et al., 2015) (*H1.0*), although there was no significant effect for 1977 or 1999 individually (Tables 1, 4). The same held true for $\ln[H]$ as a univariate predictor (*H1.1*; Tables 1, 4). When combined with other predictor variables in our multivariate models, the top models usually included an effect of $\ln[H]$, and its coefficient was consistently negative, as predicted (Tables 1, 5). We note that a non-significant positive correlation between $\ln[H]$ and R for 1999 became negative in the context of the multivariate models, again supporting *H1.1* (Table 1).

Crown position was generally correlated with H , but with substantial variation (Fig. 2d). Crown position was a much poorer predictor of R than was H (Table 4), lending little overall support to *H1.2* (Table 1). When considered alone, CP had a significant influence only in the 1966 drought, during which trees with dominant CP had the lowest R . When considered in conjunction with H , CP came out as a significant predictor only for the 1999 drought, during which suppressed and then intermediate trees had the lowest R . Crown position was included in almost half of the top models, with mixed results as to how R varied with CP (Table 5). Most commonly in these multivariate models, as in the univariate models (Table 4), the resistance of dominant trees was less than that of co-dominant trees but higher than that of suppressed trees. Thus, CP was sometimes a useful predictor of R , but overall had a weak effect relative to that of H .

In the non-drought years for which we have vertical profiles in climate data (2016-2018), taller trees—or those

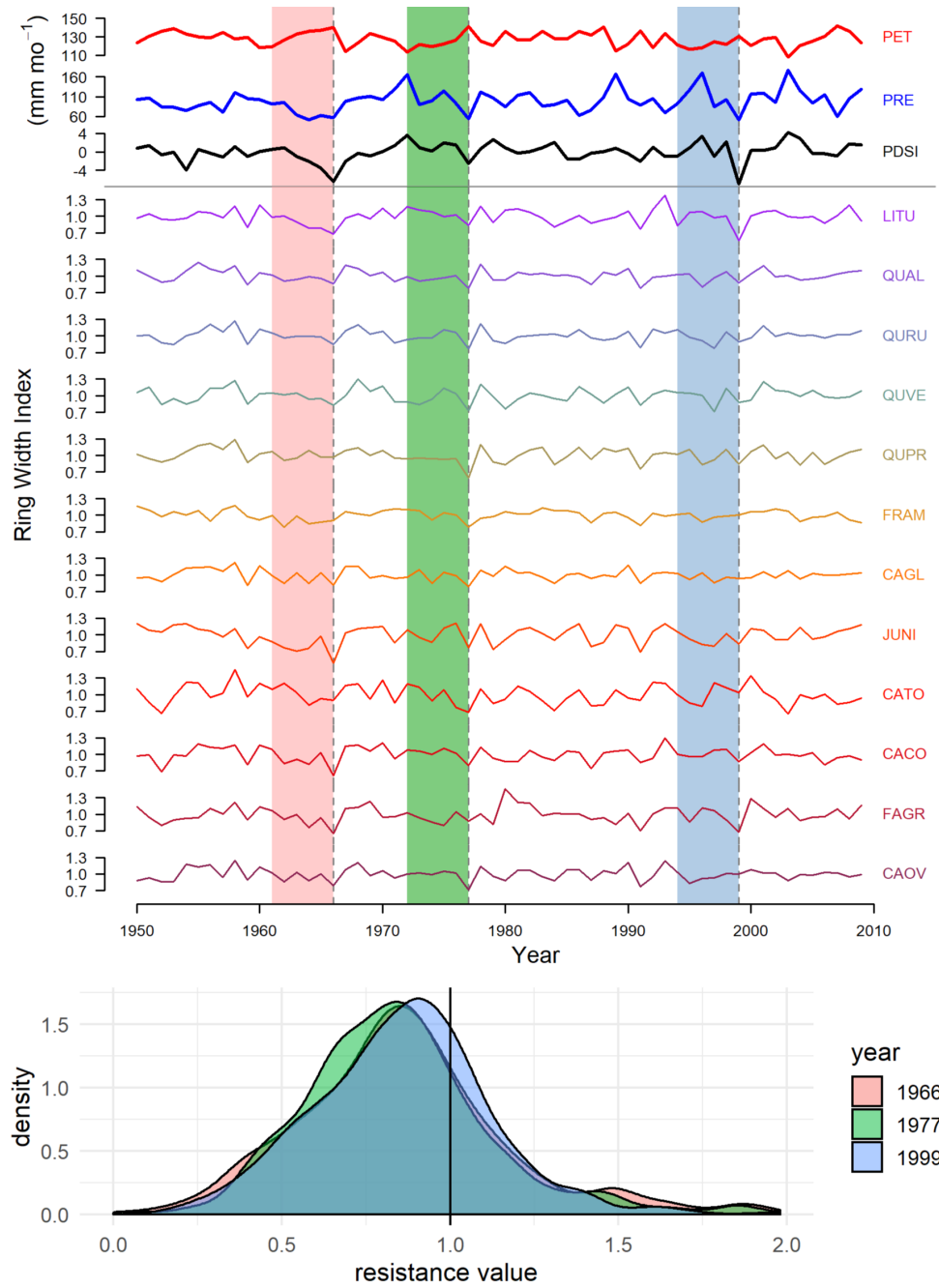


Figure 1. Climate and species-level growth responses over our study period, highlighting the three focal droughts (a) and community-wide responses Time series plot (a) shows peak growing season (May–August) climate conditions and residual chronologies for each species. Focal droughts are indicated by dashed lines, and shading indicates the pre-drought period used in calculations of the resistance metric. Figure modified from (Helcoski et al., 2019). Density plots (b) show community- wide resistance values for each drought.

Table 4. Univariate models

| variable | category | null variables | all droughts | | 1966 | | 1977 | | 1999 | |
|--------------------|-----------|-----------------|--------------|--------------|-------|--------------|-------|--------------|--------|--------------|
| | | | dAICc | coefficients | dAICc | coefficients | dAICc | coefficients | dAICc | coefficients |
| drought year | 1966 | | -2.42 | 0.0000 | - | - | - | - | - | - |
| | 1977 | | - | -0.0209 | - | - | - | - | - | - |
| | 1999 | | - | -0.0105 | - | - | - | - | - | - |
| ln[DBH] | | Y | 8.17 | -0.0385 | 15.32 | -0.0888 | -0.87 | -0.0214 | -1.93 | 0.0057 |
| ln[height] | | Y | 8.17 | -0.0620 | 15.32 | -0.143 | -0.87 | -0.0345 | -1.93 | 0.0092 |
| crown position | D | Y | -2.96 | -0.0461 | 3.25 | -0.0509 | 0.66 | -0.0759 | 0.38 | -0.0103 |
| (alone) | C | | - | 0.0000 | - | 0 | - | 0 | - | 0 |
| | I | | - | -0.0063 | - | 0.0732 | - | -0.0298 | - | -0.0563 |
| | S | | - | 0.0122 | - | 0.0526 | - | 0.0432 | - | -0.0483 |
| crown position | D | ln[H]+Y | 0.57 | -0.0347 | -1.84 | -0.0328 | -0.23 | -0.073 | 3.04 | -0.0024 |
| (with height) | C | | - | 0.0000 | - | 0 | - | 0 | - | 0 |
| | I | | - | -0.0425 | - | 0.0139 | - | -0.0388 | - | -0.081 |
| | S | | - | -0.0582 | - | -0.0662 | - | 0.0258 | - | -0.0956 |
| ln[TWI] | | ln[H]+Y | 5.34 | -0.0890 | -1.96 | -0.0171 | 5.05 | -0.1404 | 2.8 | -0.1033 |
| ln[TWI]*ln[H] | | ln[H]+ln[TWI]+Y | -0.83 | 0.0824 | -1.58 | 0.0958 | -1.47 | 0.089 | -1.9 | 0.0428 |
| wood density | | ln[H]+Y | -1.91 | -0.0479 | -1.24 | -0.2089 | -1.22 | -0.1812 | 0.22 | 0.2502 |
| leaf mass per area | | ln[H]+Y | -1.99 | 0.0003 | -1.88 | 0.0012 | -1.76 | -0.0013 | -2 | 0.0004 |
| xylem porosity | ring | ln[H]+Y | -2.68 | 0.0583 | 0.81 | 0.1542 | 0.42 | -0.1874 | 3.97 | 0.1998 |
| | semi-ring | | - | -0.0244 | - | -0.1112 | - | -0.1386 | - | 0.1493 |
| | diffuse | | - | 0.0000 | - | 0 | - | 0 | - | 0 |
| turgor loss point | | ln[H]+Y | 1.33 | -0.1777 | -1.64 | -0.1078 | 1.26 | -0.25 | 0.016 | -0.1732 |
| percent loss area | | ln[H]+Y | 7.17 | -0.0140 | 9.18 | -0.0249 | -0.05 | -0.0105 | -0.716 | -0.0074 |

Table 5. Summary of R^2 and coefficients of the best multivariate models for each drought instance. Models are ranked by AIC, and we show all models whose AIC value falls within 2.0 of the best model (dAICc<2).

| drought | dAICc | R2 | Intercept | ln[H] | crown position | | | | ln[TWI] | xylem architecture | | | PLA | TLP |
|---------|-------|------|-----------|--------|----------------|---|--------|--------|---------|--------------------|-----------|--------|--------|--------|
| | | | | | D | C | I | S | | diffuse | semi-ring | ring | | |
| all | 0.000 | 0.12 | 1.085 | -0.059 | - | - | - | - | -0.086 | - | - | - | -0.012 | -0.113 |
| | 0.371 | 0.12 | 1.401 | -0.061 | - | - | - | - | -0.087 | 0 | 0.164 | 0.049 | -0.018 | - |
| | 0.586 | 0.11 | 1.373 | -0.057 | - | - | - | - | -0.086 | - | - | - | -0.013 | - |
| | 0.726 | 0.12 | 1.232 | -0.092 | -0.034 | 0 | -0.037 | -0.051 | -0.079 | - | - | - | -0.012 | -0.101 |
| | 0.813 | 0.11 | 1.493 | -0.092 | -0.034 | 0 | -0.039 | -0.054 | -0.079 | - | - | - | -0.014 | - |
| | 1.051 | 0.13 | 1.508 | -0.095 | -0.032 | 0 | -0.038 | -0.052 | -0.08 | 0 | 0.149 | 0.051 | -0.017 | - |
| 1966 | 0.000 | 0.27 | 2.401 | -0.151 | - | - | - | - | - | 0 | 0.428 | 0.159 | -0.039 | 0.284 |
| | 0.837 | 0.27 | 1.564 | -0.151 | - | - | - | - | - | 0 | 0.142 | 0.137 | -0.025 | - |
| | 1.443 | 0.25 | 1.641 | -0.14 | - | - | - | - | - | - | - | - | -0.025 | - |
| | 1.599 | 0.27 | 2.546 | -0.176 | -0.034 | 0 | 0.012 | -0.069 | - | 0 | 0.442 | 0.162 | -0.039 | 0.31 |
| | 1.972 | 0.27 | 2.439 | -0.151 | - | - | - | - | -0.017 | 0 | 0.434 | 0.16 | -0.039 | 0.288 |
| 1977 | 0.000 | 0.22 | 0.346 | - | -0.074 | 0 | -0.027 | 0.042 | -0.131 | 0 | -0.331 | -0.23 | - | -0.384 |
| | 0.090 | 0.21 | 0.393 | - | - | - | - | - | -0.14 | 0 | -0.324 | -0.234 | - | -0.369 |
| | 1.506 | 0.22 | 0.449 | -0.023 | - | - | - | - | -0.137 | 0 | -0.314 | -0.226 | - | -0.37 |
| 1999 | 0.000 | 0.24 | 1.042 | - | - | - | - | - | -0.1 | 0 | 0.261 | 0.191 | -0.01 | - |
| | 0.123 | 0.25 | 1.280 | -0.072 | 0.004 | 0 | -0.076 | -0.091 | -0.088 | 0 | 0.242 | 0.195 | -0.009 | - |
| | 0.370 | 0.24 | 0.533 | - | - | - | - | - | -0.098 | 0 | 0.077 | 0.181 | - | -0.161 |
| | 0.913 | 0.24 | 1.143 | -0.071 | 0.002 | 0 | -0.077 | -0.092 | -0.09 | 0 | 0.146 | 0.202 | - | - |
| | 1.142 | 0.22 | 0.902 | - | - | - | - | - | -0.102 | 0 | 0.161 | 0.199 | - | - |
| | 1.485 | 0.24 | 1.153 | -0.08 | 0 | 0 | -0.081 | -0.096 | - | 0 | 0.235 | 0.196 | -0.01 | - |
| | 1.586 | 0.26 | 1.063 | - | -0.005 | 0 | -0.05 | -0.041 | -0.097 | 0 | 0.232 | 0.183 | -0.009 | - |
| | 1.714 | 0.24 | 0.645 | -0.079 | -0.001 | 0 | -0.081 | -0.095 | - | 0 | 0.054 | 0.186 | - | -0.162 |
| | 1.821 | 0.26 | 0.580 | - | -0.006 | 0 | -0.051 | -0.041 | -0.095 | 0 | 0.059 | 0.174 | - | -0.154 |
| | 1.878 | 0.25 | 0.827 | - | - | - | - | - | -0.099 | 0 | 0.187 | 0.186 | -0.006 | -0.073 |

in dominant crown positions— were generally exposed to higher evaporative demand during the peak growing season months (May–August; Fig. 2). Specifically, maximum daily wind speeds were significantly higher above the top of the canopy (40–50m) than within and below (10–30m) (Fig. 2a). Relative humidity was also somewhat lower during June–August, ranging from ~50–80 above the canopy and ~60–90% in the understory (Fig. 2b). Air temperature did not vary across the vertical profile (Fig. 2c).

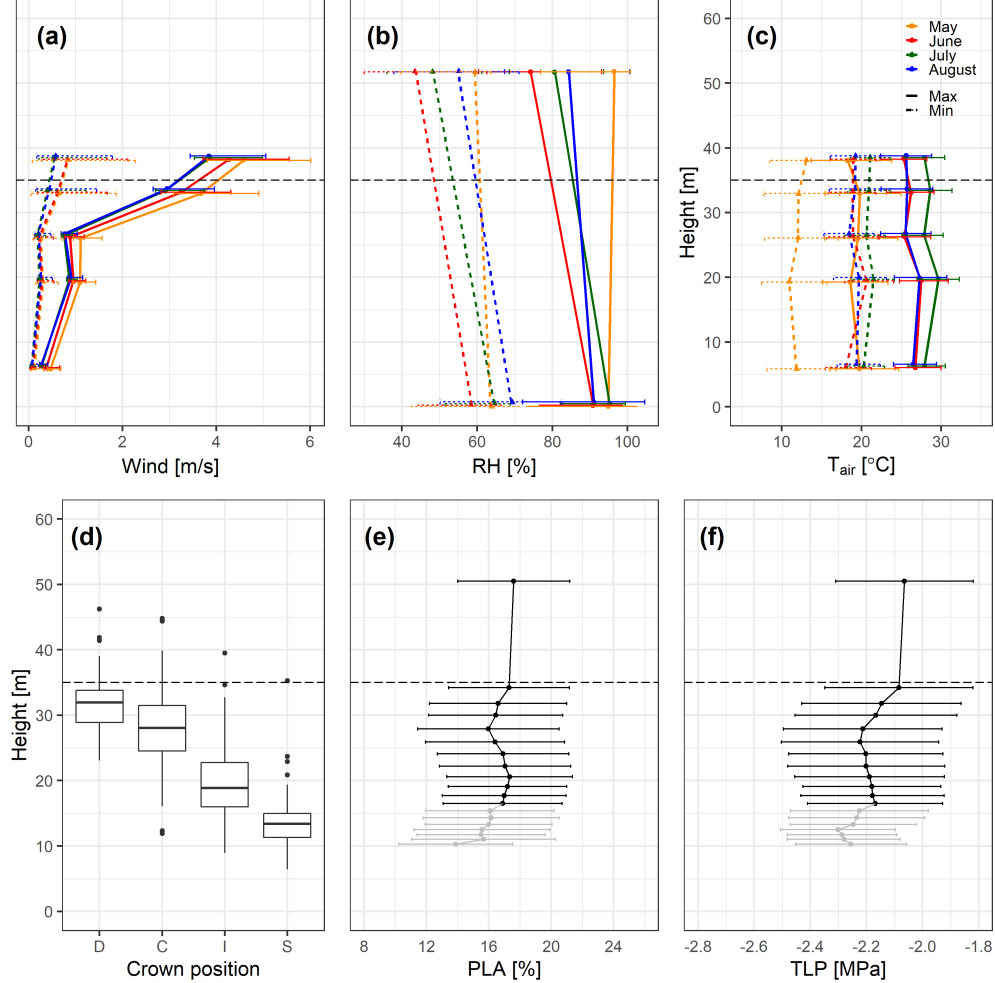


Figure 2. Height profiles in growing season climatic conditions, tree heights by crown position, and leaf hydraulic traits The top row shows averages (\pm SD) of daily maxima and minima of (a) wind speed, (b) relative humidity (RH), and (c) air temperature (T_{air}) averaged over each month of the peak growing season (May–August) from 2016–2018. In these plots, heights are slightly offset for visualization purposes. Also shown are (d) 2018 tree heights by canopy position (see Table 2 for codes) and vertical profiles in (e) PLA_{dry} and (f) π_{tlp} . In (e–f), values are community-wide averages across height bins (plotted at upper end of height bin), with grey indicating bins for which species-level trait measurements are available for <75% of individuals. In all plots, the dashed horizontal line indicates the 95th percentile of tree heights in the ForestGEO plot.

Resistance was negatively correlated with $\ln[TWI]$ (Tables 4–5), negating the idea that trees in moist microsites would suffer less during drought. Nevertheless, we tested for a negative $\ln[H] * \ln[TWI]$ interaction ($H1.3$), which could indicate that smaller trees (with smaller rooting volume) have a greater tendency to suffer more in drier microenvironments with greater depth to the water table. $H1.3$ was rejected; the $\ln[H] * \ln[TWI]$ interaction was never significant and had a consistently positive coefficient (Table 4).

Species' traits, height, and drought resistance

We partially support $H2.1$: Species' hydraulic traits – XP , PLA_{dry} , and π_{tlp} —were sometimes useful in

explaining variation in drought responses, whereas *LMA* and *WD* were not (Tables 1,4,5). Specifically, *LMA* and *WD* never significantly associated with *R* in the univariate models (all $\text{dAIC} \leq 0.22$; Table 4), and therefore these were excluded as candidate variables for the full multivariate models. In contrast, *XP*, *PLA_{dry}*, and π_{tlp} all explained at least modest amounts of variation ($\text{dAIC} > 1.0$) in at least one drought (Table 4). Of these, *PLA_{dry}* was the strongest predictor, with consistently negative coefficients across all droughts. π_{tlp} never came out as significant ($\text{dAIC} \geq 2$) in the univariate models, but had a consistently negative coefficient (Table 4). Whereas ring-porous species had highest *R* overall and in the 1966 and 1999 droughts, they had lower *R* in 1977. Results were similar in the context of multivariate models (Table 5), except that π_{tlp} had a positive coefficient in the 1966 models in which it was included.

We reject *H2.2*, finding no evidence that taller trees tend to have traits associated with greater drought resistance. In part because of the large sample size ($n = \#$ trees—all individuals of our 12 focal species ≥ 10 cm in 25.6 ha), there were very significant ($p < 0.0001$) correlations of *H* with all species' traits (see Table S4). However, the correlation only matched the predicted direction (*i.e.*, more drought-resistant traits associated to taller trees) in the cases of *WD* *LMA*, which were not useful predictors of *R*. Furthermore, although correlations were statistically significant, trait variation within each height class overwhelmed any vertical trends (Fig. 2e-f).

We support the hypothesis (*H2.3*) that the observed tendency for larger trees to have greater growth reductions during drought (lower *R*) is driven by height itself, as opposed to more drought-sensitive traits in larger trees (Tables 1,5). As discussed above, there was little meaningful variation in traits with height at the community level. When $\ln[H]$ and hydraulic traits were considered together in multivariate models, the effect of $\ln[H]$ on *R* was consistently negative (Table 5)—reversing a non-significant positive $\ln[H]$ -*R* correlation in the univariate model for the 1999 drought (Table 4).

Responses across droughts

We reject the hypothesis (*H3.1*) that overall community responses varied across droughts. Within the context of mixed effects models, there were no significant differences in *R* across drought years (Table 4). This is consistent with the observation that the distribution of *R* values was similar across droughts (Fig. 1b).

We mostly reject the hypothesis (*H3.2*) that directions of responses varied across droughts. In the majority of cases, response directions were consistent across droughts in both univariate and multivariate models (Tables 1,4,5). However, there were a few exceptions—most commonly in the categorical variables (*CP* and *XP*) but also for π_{tlp} in the multivariate model for the 1966 drought; Tables 4, 5). These differences may very well be random, as opposed to statistically meaningful. Among the univariate models, there was no instance where predictor variables significantly improved the models of two different droughts ($\text{dAIC} \geq 2$), but with contrasting coefficients (Table 4). Among the multivariate models, *CP* was not consistently in the top models for any drought (Table 5), and π_{tlp} only appeared with a positive coefficient in two of five models for the 1966 drought (contrasting with a negative coefficient in the univariate model; Table 4). The difference most likely to be real is that ring and semi-ring porous species had lower resistance than diffuse porous species in the 1977 drought, contrasting with higher resistance in 1966 and 1999 (Tables 4,5), but note that *XP* was not a significant predictor on its own for the 1977 drought.

We support the hypothesis (*H3.3*) that the strength of predictor variables was different across the droughts (Tables 1,4,5). For instance, $\ln[H]$ and *PLA_{dry}* had much stronger negative effects in 1966 than in the other two years, $\ln[TWI]$ had the strongest negative effect in 1977, and *CP* (lowest *R* among suppressed trees) and *XP* (lowest *R* among diffuse-porous trees) were strongest in 1999 (Tables 4,5).

Discussion

Our results reveal how tree size, microhabitat, and hydraulic traits shaped tree growth responses across three droughts in a temperate deciduous forest (Table 1). The tendency for larger trees to suffer more, observed here as in forests around the world (Bennett et al., 2015), was driven primarily by their height. There was a marginal additional effect of crown exposure, with the most exposed and the most suppressed trees suffering most—consistent with observations of both greater drought sensitivity of exposed trees (*e.g.*, Suarez et al., 2004); (Scharnweber et al., 2019)) and greater sensitivity of suppressed and crowded individuals (**REFS**).

There was no evidence that root water access increased drought resistance; in contrast, trees in wetter topographic positions suffered more (consistent with (Zuleta et al., 2017)), and larger rooting volume provided no advantage in the drier microenvironments. The lower drought resistance of larger trees was not driven by any tendency for the canopy to be dominated by more drought-sensitive species. Drought-sensitive species were not linked to LMA and WD but were predicted—at least some of the time—by hydraulic traits (PLA_{dry} , π_{tlp} , and XP), which is physiologically logical ((Scoffoni et al., 2014);(Bartlett et al., 2016); (Medeiros et al., 2019)) but scientifically novel in that PLA_{dry} and π_{tlp} have not previously been linked to drought growth responses. The direction of these responses was mostly consistent across droughts, indicating that they were driven by fundamental physiological mechanisms; however, the strengths of each predictor varied across droughts, indicating that specific drought characteristics interact with tree size, microenvironment, and traits to shape which individuals suffer most. These findings significantly advance our knowledge as to the factors that confer vulnerability or resilience on trees during drought.

The droughts considered here were of similar severity (Fig. 1b) and fairly moderate; droughts of this magnitude have occurred with an average frequency of approximately one per 10-15 years (Fig. 1a, Helcoski et al. (2019)). Therefore, we expect that most species are adapted, and individual trees acclimatized, to survive droughts of this nature. While the majority of trees experienced reduced growth, a substantial portion had increased growth (Fig. 1b), underlining the fact that these droughts did not induce extreme stress on the entire forest. It is likely for this reason, combined with the fact that many factors other than climate affect tree growth in closed-canopy forests, that our best models characterize only a modest amount of variation: 11-13% for all droughts combined, and 21-27% for each individual drought (Table 5). Methodologically, the moderate nature of these droughts is an advantage because our analysis considers only trees that survived all of these droughts, and we lack information on the trees that were killed. These are likely to be relatively modest in number, and local forest monitoring data stretching back to the late 1980s confirms that the 1999 drought did not trigger major declines in tree abundance or biomass (*Anderson-Teixeira et al., in review*). Thus, the droughts considered here are substantially weaker than those that have triggered massive tree die-off (e.g., (Allen et al., 2010)), many of which have shaped our understanding about the role of tree size (Bennett et al., 2015; Stovall et al., 2019) and—to some extent—traits (Greenwood et al. (2017); Anderegg et al. (2016)). Nevertheless, our results are consistent with findings from more extreme droughts.

Our analysis indicates that height—as opposed to canopy position or root water access—is the primary factor through which tree size mediates drought response. Taller trees face inherent biophysical challenges in lifting water a greater distance against the effects of gravity and friction (Ryan et al., 2006; McDowell and Allen, 2015; McDowell et al., 2011; Couvreur et al., 2018). Vertical gradients in stem and leaf hydraulic traits—including smaller and thicker (higher LMA) leaves, more negative $P50$, and lower hydraulic conductivity at greater heights (Couvreur et al., 2018; Koike et al., 2001; McDowell et al., 2011)—make it biophysically possible for trees to become tall (Couvreur et al., 2018), yet height becomes a liability when drought incurs additional hydraulic challenges. Taller trees also face different microenvironments (Fig. 2a-b), in part because they are more likely to be in dominant canopy positions (Fig. 2d). Even under non-drought conditions, evaporative demand increases with tree height, and tall trees are more closely coupled to the atmosphere (**REFS- Jarvis 1984?**; (Bretfeld et al., 2018)). Exposed canopy leaves reach higher temperatures (**REFS**), particularly during drought when solar radiation tends to be higher and less water is available for evaporative cooling of the leaves. Furthermore, daytime CO_2 concentrations tend to decrease with height (Koike et al., 2001), implying that water costs of CO_2 uptake increase with height. Correlation between height and canopy position (Fig. 2d) makes it challenging to disentangle the relative importance of height *per se* from microenvironment. However, significant decoupling between height and canopy position can be introduced by the configuration of neighboring trees (Fig. 2d) (Muller-Landau et al., 2006), and we show that height is a far stronger predictor of drought response than crown position (Tables 1,4,5). Our analysis does have the limitation that canopy positions were recored in 2018 and undoubtedly changed for some trees since the 1960s, and we note that CP became an increasingly poor predictor moving from 1999 back to 1966 (Table 4). However, because trees would generally advance towards more dominant positions as they grow and as neighbors die, changing canopy positions would bias against the acceptance of $H1.2$. The implication is that dominant crown positions did have a marginally negative influence on R , which makes sense in light of the vertical environmental gradients described above and agrees with previous studies showing greater drought sensitivity in more exposed trees ((Suarez et al., 2004); (Scharnweber et al., 2019)).

It is safe to assume that currently suppressed trees have always been suppressed, and their relatively low R (after correcting for height effects) is real, which is consistent with analyses showing that suppressed—and particularly crowded—trees can suffer disproportionately during drought (**REFS**). The observed height-sensitivity of R , together with the apparent lack of importance of root water access (*H1.3*), agrees with the concept that physiological limitations to transpiration under drought shift from root water access to the plant-atmosphere interface as forests age (Bretfeld et al., 2018), such that tall trees—particularly the very tallest—are the most sensitive in mature forests. Additional research comparing drought responses of young and old forest stands, along with and short and tall isolated trees, would be valuable for more clearly disentangling the roles of tree height and crown exposure.

The development of tree-ring chronologies for all dominant tree species at our site (Helcoski et al., 2019) made it possible to compare historical drought responses across 12 species and their associated traits at a single site for the first time (**verify- Neil, Alan**). Concerted measurement of leaf hydraulic traits of emerging importance (Scoffoni et al., 2014; Bartlett et al., 2016; Medeiros et al., 2019) allowed novel insights into the role of hydraulic traits in shaping drought response. The finding that PLA_{dry} and π_{tlp} can be useful for predicting drought responses is consistent with studies demonstrating that these are physiologically meaningful traits linked to species distribution along moisture gradients (Medeiros et al., 2019) (**MORE REFS-KAT/NOBBY/LAWREN**), **MORE-KAT/NOBBY/LAWREN...** (**REFS**). It is scientifically exciting in that it indicates that PLA_{dry} and π_{tlp} , which can be measured relatively easily (Bartlett et al., 2012; Scoffoni et al., 2014), hold promise for predicting drought growth responses across species. The importance of linking species' traits to drought responses increases with tree species diversity; whereas it is feasible to study drought responses for all dominant species in most boreal and temperate forests (e.g., this study), this becomes difficult to impossible for diverse tropical forests, where linking hydraulic traits to drought responses would be invaluable for forecasting how little-known species and whole forests will respond to future droughts (**REFS-KAT/NOBBY/LAWREN**).

Our analysis of hydraulic traits focused on species-level comparisons and did not characterize the role of variation with height. As noted above, leaves found higher on a tree tend to have more hydraulically conservative traits, and therefore we would expect that average leaf characteristics of an individual tree would scale with its crown height, with taller individuals having on average more drought-resistant traits. If vertical trends for PLA_{dry} and π_{tlp} , which have not been characterized (**LAWREN, IS THIS TRUE?**), *follow the general pattern of increasing leaf drought resistance with height, our analysis would be biased in a conservative direction when assessing H2.3** (Table 1)—i.e., accounting traits on an individual level should result in a stronger negative effect of $\ln[H]$. Further characterization of leaf hydraulic traits in relation to height and crown exposure would be valuable for enhancing our understanding of the interactive effects of tree height and traits on drought responses.

Although the physiological mechanisms discussed above lead to generally consistent directions of growth responses to tree height and hydraulic traits across droughts, indicating the universality of the underlying mechanisms, the relative importance of the drivers varied widely across droughts, indicating an interaction with drought characteristics (Tables 4-5). Although there were not significant differences in R among the drought years, R tended to be somewhat lower in 1966 (Fig. 1, Table 4). Height and dominant canopy position had the stronger negative effects in this drought than in the others (Tables 4-5), consistent with the finding that height becomes a stronger predictor of mortality as the severity of the drought increases (Stovall et al., 2019). In 1977, which was the weakest drought (Fig. S3, Table S2), the only factor useful for predicting R in the univariate models was microhabitat moisture (TWI , Table 4). Somewhat surprisingly, but consistent with the weakening drought sensitivity observed by (Helcoski et al., 2019), the highest overall R was observed during the 1999 drought, which was the most intense and second-longest in duration. For this drought, xylem architecture was the most useful predictor, with diffuse-porous species suffering most. Thus, responses differed with the nature of each drought. Of course, site characteristics also define the nature of droughts, and comparisons of size and trait effects across sites—and across more droughts at a single site—would be of great value to elucidating the mechanisms through which drought characteristics interact with driver variables to shape tree growth responses.

As climate change drives increasing drought in many of the world's forests (**REFS-KAT**), the fate of forests and their climate feedbacks will be shaped by the biophysical and physiological drivers observed here. Large

trees have been suffering disproportionately in forests around the world (Bennett et al., 2015; Stovall et al., 2019), and we here show that this is primarily driven by their height, with some contributions from canopy position. The distinction is important because it suggests that height *per se* makes trees vulnerable, even if their crowns are somewhat protected by neighbors, whereas solitary trees or the dominant trees in young regrowth forests should be less vulnerable. Considering just height and crown position, this would suggest that mature forests would be more vulnerable to drought than young forests with short trees; however, root water access may limit the young forests (*Bretfield et al.*), and species traits often shift as forests age, with early successional species tending to have lower wood densities and higher hydraulic conductivities that facilitate rapid growth (**REFS in Bretfield-beginning of discussion**). Pioneer species at our site (*Liriodendron tulipifera*, *Quercus spp.*, *Fraxinus americana*) have a mix of traits conferring drought tolerance and resistance (Table 3), and further research on how hydraulic traits and drought vulnerability change over the course of succession would be valuable for getting at the very significant question of whether old-growth forests are more vulnerable to drought, and to which types of drought. In the meantime, the results of this study advance our knowledge of the factors conferring drought vulnerability and resistance in a mature forest, opening the door for more accurate forecasting of forest responses to future drought.

Acknowledgements

funding: ForestGEO,

Author Contribution

words

References

- Abrams, M. D. (1990). Adaptations and responses to drought in *Quercus* species of North America. *Tree Physiology*, 7(1-2-3-4):227–238.
- Allen, C. D., Macalady, A. K., Chenchouni, H., Bachelet, D., McDowell, N., Vennetier, M., Kitzberger, T., Rigling, A., Breshears, D. D., Hogg, E. H. T., Gonzalez, P., Fensham, R., Zhang, Z., Castro, J., Demidova, N., Lim, J.-H., Allard, G., Running, S. W., Semerci, A., and Cobb, N. (2010). A global overview of drought and heat-induced tree mortality reveals emerging climate change risks for forests. *Forest Ecology and Management*, 259(4):660–684.
- Anderegg, W. R. L., Klein, T., Bartlett, M., Sack, L., Pellegrini, A. F. A., Choat, B., and Jansen, S. (2016). Meta-analysis reveals that hydraulic traits explain cross-species patterns of drought-induced tree mortality across the globe. *Proceedings of the National Academy of Sciences*, 113(18):5024–5029.
- Anderegg, W. R. L., Konings, A. G., Trugman, A. T., Yu, K., Bowling, D. R., Gabbitas, R., Karp, D. S., Pacala, S., Sperry, J. S., Sulman, B. N., and Zenes, N. (2018). Hydraulic diversity of forests regulates ecosystem resilience during drought. *Nature*, 561(7724):538–541.
- Anderson-Teixeira, K. J., Davies, S. J., Bennett, A. C., Gonzalez-Akre, E. B., Muller-Landau, H. C., Wright, S. J., Salim, K. A., Zambrano, A. M. A., Alonso, A., Baltzer, J. L., Basset, Y., Bourg, N. A., Broadbent, E. N., Brockelman, W. Y., Bunyavechewin, S., Burslem, D. F. R. P., Butt, N., Cao, M., Cardenas, D., Chuyong, G. B., Clay, K., Cordell, S., Dattaraja, H. S., Deng, X., Detto, M., Du, X., Duque, A., Erikson, D. L., Ewango, C. E. N., Fischer, G. A., Fletcher, C., Foster, R. B., Giardina, C. P., Gilbert, G. S., Gunatilleke, N., Gunatilleke, S., Hao, Z., Hargrove, W. W., Hart, T. B., Hau, B. C. H., He, F., Hoffman, F. M., Howe, R. W., Hubbell, S. P., Inman-Narahari, F. M., Jansen, P. A., Jiang, M., Johnson, D. J., Kanzaki, M., Kassim, A. R., Kenfack, D., Kibet, S., Kinnaird, M. F., Korte, L., Kral, K., Kumar, J., Larson, A. J., Li, Y., Li, X., Liu, S., Lum, S. K. Y., Lutz, J. A., Ma, K., Maddalena, D. M., Makana, J.-R., Malhi, Y., Marthens, T., Serudin, R. M., McMahon, S. M., McShea, W. J., Memiaghe, H. R., Mi, X., Mizuno, T., Morecroft, M., Myers, J. A., Novotny, V., Oliveira, A. A. d., Ong, P. S., Orwig, D. A., Ostertag, R., Ouden, J. d., Parker, G. G., Phillips, R. P., Sack, L., Sainge, M. N., Sang, W., Sri-ngernyuan, K., Sukumar, R., Sun, I.-F., Sungpalee, W., Suresh, H. S., Tan, S., Thomas, S. C., Thomas, D. W., Thompson, J., Turner, B. L., Uriarte, M., Valencia, R., Vallejo, M. I., Vicentini, A., Vřška, T., Wang, X., Wang, X., Weiblen, G., Wolf, A., Xu, H., Yap, S., and Zimmerman, J. (2015a). CTFS-ForestGEO: a worldwide network monitoring forests in an era of global change. *Global Change Biology*, 21(2):528–549.
- Anderson-Teixeira, K. J., McGarvey, J. C., Muller-Landau, H. C., Park, J. Y., Gonzalez-Akre, E. B., Herrmann, V., Bennett, A. C., So, C. V., Bourg, N. A., Thompson, J. R., McMahon, S. M., and McShea, W. J. (2015b). Size-related scaling of tree form and function in a mixed-age forest. *Functional Ecology*, 29(12):1587–1602.
- Bartlett, M. K., Klein, T., Jansen, S., Choat, B., and Sack, L. (2016). The correlations and sequence of plant stomatal, hydraulic, and wilting responses to drought. *Proceedings of the National Academy of Sciences*, 113(46):13098–13103.
- Bartlett, M. K., Scoffoni, C., Ardy, R., Zhang, Y., Sun, S., Cao, K., and Sack, L. (2012). Rapid determination of comparative drought tolerance traits: using an osmometer to predict turgor loss point. *Methods in Ecology and Evolution*, 3(5):880–888.
- Bennett, A. C., McDowell, N. G., Allen, C. D., and Anderson-Teixeira, K. J. (2015). Larger trees suffer most during drought in forests worldwide. *Nature Plants*, 1(10):15139.
- Beven, K. J. and Kirkby, M. J. (1979). A physically based, variable contributing area model of basin hydrology / Un modèle à base physique de zone d’appel variable de l’hydrologie du bassin versant. *Hydrological Sciences Bulletin*, 24(1):43–69.
- Bonan, G. B. (2008). Forests and Climate Change: Forcings, Feedbacks, and the Climate Benefits of Forests. *Science*, 320(5882):1444–1449.

- Bourg, N. A., McShea, W. J., Thompson, J. R., McGarvey, J. C., and Shen, X. (2013). Initial census, woody seedling, seed rain, and stand structure data for the SCBI SIGEO Large Forest Dynamics Plot. *Ecology*, 94(9):2111–2112.
- Bretfeld, M., Ewers, B. E., and Hall, J. S. (2018). Plant water use responses along secondary forest succession during the 2015–2016 El Niño drought in Panama. *New Phytologist*, 219(3):885–899.
- Condit, R. (1998). *Tropical Forest Census Plots: Methods and Results from Barro Colorado Island, Panama and a Comparison with Other Plots*. Springer Berlin Heidelberg, Berlin, Heidelberg.
- Condit, R., Watts, K., Bohlman, S. A., Pérez, R., Foster, R. B., and Hubbell, S. P. (2000). Quantifying the deciduousness of tropical forest canopies under varying climates. *Journal of Vegetation Science*, 11(5):649–658.
- Couvreur, V., Ledder, G., Manzoni, S., Way, D. A., Muller, E. B., and Russo, S. E. (2018). Water transport through tall trees: A vertically explicit, analytical model of xylem hydraulic conductance in stems. *Plant, Cell & Environment*, 41(8):1821–1839.
- D’Orangeville, L., Maxwell, J., Kneeshaw, D., Pederson, N., Duchesne, L., Logan, T., Houle, D., Arseneault, D., Beier, C. M., Bishop, D. A., Druckenbrod, D., Fraver, S., Girard, F., Halman, J., Hansen, C., Hart, J. L., Hartmann, H., Kaye, M., Leblanc, D., Manzoni, S., Ouimet, R., Rayback, S., Rollinson, C. R., and Phillips, R. P. (2018). Drought timing and local climate determine the sensitivity of eastern temperate forests to drought. *Global Change Biology*, 24(6):2339–2351.
- Elliott, K. J., Miniati, C. F., Pederson, N., and Laseter, S. H. (2015). Forest tree growth response to hydroclimate variability in the southern Appalachians. *Global Change Biology*, 21(12):4627–4641.
- Friedlingstein, P., Cox, P., Betts, R., Bopp, L., von Bloh, W., Brovkin, V., Cadule, P., Doney, S., Eby, M., Fung, I., Bala, G., John, J., Jones, C., Joos, F., Kato, T., Kawamiya, M., Knorr, W., Lindsay, K., Matthews, H. D., Raddatz, T., Rayner, P., Reick, C., Roeckner, E., Schnitzler, K.-G., Schnur, R., Strassmann, K., Weaver, A. J., Yoshikawa, C., and Zeng, N. (2006). Climate–Carbon Cycle Feedback Analysis: Results from the C4mip Model Intercomparison. *Journal of Climate*, 19(14):3337–3353.
- Friedrichs, D. A., Trouet, V., Büntgen, U., Frank, D. C., Esper, J., Neuwirth, B., and Löffler, J. (2009). Species-specific climate sensitivity of tree growth in Central-West Germany. *Trees*, 23(4):729.
- Gonzalez-Akre, E., Meakem, V., Eng, C.-Y., Tepley, A. J., Bourg, N. A., McShea, W., Davies, S. J., and Anderson-Teixeira, K. (2016). Patterns of tree mortality in a temperate deciduous forest derived from a large forest dynamics plot. *Ecosphere*, 7(12):e01595.
- Greenwood, S., Ruiz-Benito, P., Martínez-Vilalta, J., Lloret, F., Kitzberger, T., Allen, C. D., Fensham, R., Laughlin, D. C., Kattge, J., Bönisch, G., Kraft, N. J. B., and Jump, A. S. (2017). Tree mortality across biomes is promoted by drought intensity, lower wood density and higher specific leaf area. *Ecology Letters*, 20(4):539–553.
- Guerfel, M., Baccouri, O., Boujnah, D., Chaïbi, W., and Zarrouk, M. (2009). Impacts of water stress on gas exchange, water relations, chlorophyll content and leaf structure in the two main Tunisian olive (*Olea europaea* L.) cultivars. *Scientia Horticulturae*, 119(3):257–263.
- Hacket-Pain, A. J., Cavin, L., Friend, A. D., and Jump, A. S. (2016). Consistent limitation of growth by high temperature and low precipitation from range core to southern edge of European beech indicates widespread vulnerability to changing climate. *European Journal of Forest Research*, 135(5):897–909.
- Harris, I., Jones, P. D., Osborn, T. J., and Lister, D. H. (2014). Updated high-resolution grids of monthly climatic observations – the CRU TS3.10 Dataset. *International Journal of Climatology*, 34(3):623–642.
- Helcoski, R., Tepley, A. J., Pederson, N., McGarvey, J. C., Meakem, V., Herrmann, V., Thompson, J. R., and Anderson-Teixeira, K. J. (2019). Growing season moisture drives interannual variation in woody productivity of a temperate deciduous forest. *New Phytologist*, 0(0).

- Hoffmann, W. A., Marchin, R. M., Abit, P., and Lau, O. L. (2011). Hydraulic failure and tree dieback are associated with high wood density in a temperate forest under extreme drought. *Global Change Biology*, 17(8):2731–2742.
- Intergovernmental Panel on Climate Change (2015). *Climate Change 2014: Impacts, Adaptation and Vulnerability: Working Group II Contribution to the IPCC Fifth Assessment Report. Volume 2 Volume 2*. OCLC: 900892773.
- Jennings, S. B., Brown, N. D., and Sheil, D. (1999). Assessing forest canopies and understorey illumination: canopy closure, canopy cover and other measures. *Forestry: An International Journal of Forest Research*, 72(1):59–74.
- Kannenberg, S. A., Novick, K. A., Alexander, M. R., Maxwell, J. T., Moore, D. J. P., Phillips, R. P., and Anderegg, W. R. L. (2019). Linking drought legacy effects across scales: From leaves to tree rings to ecosystems. *Global Change Biology*, 0(ja).
- Koike, T., Kitao, M., Maruyama, Y., Mori, S., and Lei, T. T. (2001). Leaf morphology and photosynthetic adjustments among deciduous broad-leaved trees within the vertical canopy profile. *Tree Physiology*, 21(12-13):951–958.
- Larjavaara, M. and Muller-Landau, H. C. (2013). Measuring tree height: a quantitative comparison of two common field methods in a moist tropical forest. *Methods in Ecology and Evolution*, 4(9):793–801.
- Lloret, F., Keeling, E. G., and Sala, A. (2011). Components of tree resilience: effects of successive low-growth episodes in old ponderosa pine forests. *Oikos*, 120(12):1909–1920.
- McDowell, N. G. and Allen, C. D. (2015). Darcy’s law predicts widespread forest mortality under climate warming. *Nature Climate Change*, 5(7):669–672.
- McDowell, N. G., Bond, B. J., Dickman, L. T., Ryan, M. G., and Whitehead, D. (2011). Relationships Between Tree Height and Carbon Isotope Discrimination. In Meinzer, F. C., Lachenbruch, B., and Dawson, T. E., editors, *Size- and Age-Related Changes in Tree Structure and Function*, Tree Physiology, pages 255–286. Springer Netherlands, Dordrecht.
- Meakem, V., Tepley, A. J., Gonzalez-Akre, E. B., Herrmann, V., Muller-Landau, H. C., Wright, S. J., Hubbell, S. P., Condit, R., and Anderson-Teixeira, K. J. (2018). Role of tree size in moist tropical forest carbon cycling and water deficit responses. *New Phytologist*, 219(3):947–958.
- Medeiros, C. D., Scoffoni, C., John, G. P., Bartlett, M. K., Inman-Narahari, F., Ostertag, R., Cordell, S., Giardina, C., and Sack, L. (2019). An extensive suite of functional traits distinguishes Hawaiian wet and dry forests and enables prediction of species vital rates. *Functional Ecology*, 33(4):712–734.
- Muller-Landau, H. C., Condit, R. S., Chave, J., Thomas, S. C., Bohlman, S. A., Bunyavejchewin, S., Davies, S., Foster, R., Gunatilleke, S., Gunatilleke, N., Harms, K. E., Hart, T., Hubbell, S. P., Itoh, A., Kassim, A. R., LaFrankie, J. V., Lee, H. S., Losos, E., Makana, J.-R., Ohkubo, T., Sukumar, R., Sun, I.-F., Nur Supardi, M. N., Tan, S., Thompson, J., Valencia, R., Muñoz, G. V., Wills, C., Yamakura, T., Chuyong, G., Dattaraja, H. S., Esufali, S., Hall, P., Hernandez, C., Kenfack, D., Kiratiprayoon, S., Suresh, H. S., Thomas, D., Vallejo, M. I., and Ashton, P. (2006). Testing metabolic ecology theory for allometric scaling of tree size, growth and mortality in tropical forests. *Ecology Letters*, 9(5):575–588.
- Pfeifer, E. M., Hicke, J. A., and Meddens, A. J. H. (2011). Observations and modeling of aboveground tree carbon stocks and fluxes following a bark beetle outbreak in the western United States. *Global Change Biology*. 17: 339-350, 17:339–350.
- Ryan, M. G., Phillips, N., and Bond, B. J. (2006). The hydraulic limitation hypothesis revisited. *Plant, Cell & Environment*, 29(3):367–381.
- Scharnweber, T., Heinze, L., Cruz-García, R., van der Maaten-Theunissen, M., and Wilmking, M. (2019). Confessions of solitary oaks: We grow fast but we fear the drought. *Dendrochronologia*, 55:43–49.

- Scoffoni, C., Vuong, C., Diep, S., Cochard, H., and Sack, L. (2014). Leaf Shrinkage with Dehydration: Coordination with Hydraulic Vulnerability and Drought Tolerance. *Plant Physiology*, 164(4):1772–1788.
- Slette, I. J., Post, A. K., Awad, M., Even, T., Punzalan, A., Williams, S., Smith, M. D., and Knapp, A. K. (2019). How ecologists define drought, and why we should do better. *Global Change Biology*, 0(0):1–8.
- Stovall, A. E. L., Anderson-Teixeira, K. J., and Shugart, H. H. (2018a). Assessing terrestrial laser scanning for developing non-destructive biomass allometry. *Forest Ecology and Management*, 427:217–229.
- Stovall, A. E. L., Anderson-Teixeira, K. J., and Shugart, H. H. (2018b). Terrestrial LiDAR-derived non-destructive woody biomass estimates for 10 hardwood species in Virginia. *Data in Brief*, 19:1560–1569.
- Stovall, A. E. L., Shugart, H., and Yang, X. (2019). Tree height explains mortality risk during an intense drought. *Nature Communications*, 10(1):1–6.
- Suarez, M. L., Ghermandi, L., and Kitzberger, T. (2004). Factors predisposing episodic drought-induced tree mortality in Nothofagus– site, climatic sensitivity and growth trends. *Journal of Ecology*, 92(6):954–966.
- Sørensen, R., Zinko, U., and Seibert, J. (2006). On the calculation of the topographic wetness index: evaluation of different methods based on field observations. *Hydrology and Earth System Sciences*, 10(1):101–112.
- Trenberth, K. E., Dai, A., van der Schrier, G., Jones, P. D., Barichivich, J., Briffa, K. R., and Sheffield, J. (2014). Global warming and changes in drought. *Nature Climate Change*, 4(1):17–22.
- Zhang, Y.-J., Meinzer, F. C., Hao, G.-Y., Scholz, F. G., Bucci, S. J., Takahashi, F. S. C., Villalobos-Vega, R., Giraldo, J. P., Cao, K.-F., Hoffmann, W. A., and Goldstein, G. (2009). Size-dependent mortality in a Neotropical savanna tree: the role of height-related adjustments in hydraulic architecture and carbon allocation. *Plant, Cell & Environment*, 32(10):1456–1466.
- Zuleta, D., Duque, A., Cardenas, D., Muller-Landau, H. C., and Davies, S. J. (2017). Drought-induced mortality patterns and rapid biomass recovery in a terra firme forest in the Colombian Amazon. *Ecology*, 98(10):2538–2546.